J Therm Spray Tech
https://doi.org/10.1007/s11666-024-01833-0

ORIGINAL RESEARCH ARTICLE

Generating Oxide-free Molten Metal Droplets by Air Plasma Spraying Enabled by Deoxidizer Addition to the Feedstock Powders

Chang-Jiu Li[1] · Xiao-Tao Luo[1] · Xin-Yuan Dong[1] · Li Zhang[1] · Yong-Sheng Zhu[1] · Cheng-Xin Li[1] · Guan-Jun Yang[1]

Submitted: 21 February 2024 / in revised form: 17 August 2024 / Accepted: 24 August 2024
© ASM International 2024

Abstract Thermal spray metallic coatings usually present a lamellar structure with limited lamellar interface bonding due to inevitable oxidation involved. Such microstructure not only degrades the mechanical performances of the coatings significantly but also cannot provide effective corrosion protection to the substrate. In the present paper, the recent progresses to generate oxide-free molten metallic droplets by air plasma spraying will be summarized toward to deposition of highly dense metal coatings. It is revealed that by designing the metallic spray powders containing deoxidizers such as boron or carbon based on thermodynamics theory of oxidation, the oxide-free in-flight molten metal droplets can be created in open atmosphere during air plasma spraying. The thermodynamics and kinetics for the in-flight deoxidization are presented for the deoxidizers of boron and carbon. The tests with Ni-based and Cu-based alloy coatings using boron as deoxidizer showed that the oxygen content in the coatings can be reduced to less than 0.6 wt.%. It was demonstrated with NiCrAlY, NiAl and FeAl alloys that contain element Al the coatings with low oxide contents can be deposited by APS using carbon as deoxidizer. The post-impact oxidation is mainly responsible for the introduction of oxide inclusions in these coatings. Besides deoxidizer addition, ultra-high temperature is the other necessary condition for the generation of oxide-free molten droplets. It was revealed that a minimum deoxidizer content is necessary to maintain continuous oxidation protection of alloying elements along with rapid mass transfer mechanism within molten metal droplets during the whole spray distance.

Keywords air plasma spraying · in situ deoxidization · metal spraying · oxide-free molten droplet

Introduction

Thermal spraying processes have been developed in the last century for a variety of industrial applications (Ref 1-3). Among different types of coatings including metals, ceramics and cermets, thermal spraying of metal coatings has the longest history since it has accompanied the growth of thermal spray technologies from its very beginning (Ref 1-2). Despite having the longest history, the prevention of the oxidation of molten metal droplets during their in-flight in an open air is still challenging and this problem has not been solved yet since oxide inclusions into the coating greatly degrade the coating performance (Ref 4). Firstly, oxide inclusions significantly reduce the wettability of spreading melt and prevent the direct contact of the flattening liquid metal with the solid metal substrate. Thus, the formation of metallurgical bonding between metal splats is hindered. The adhesion and cohesion of the metal coatings are also limited to tens of MPa by the oxide inclusions (Ref

This article is an invited paper selected from presentations at the Asian Thermal Spray Conference and Expo 2023, held November 2–4, 2023, IIT Madras, Chennai, India, and has been expanded from the original presentation. The issue was organized by Dr. Satish Tailor, Metallizing Equipment Company, Jodhpur; Prof. Srinivasa Bakshi, IITM Chennai; Prof. M. Kamaraj, IITM, Chennai; Dr. Sisir Mantry, CSIR-Institute of Minerals and Materials Technology; Dr. Andrew Ang, Swinburne University of Technology; Prof. Shrikant Joshi, University West.

✉ Chang-Jiu Li
licj@mail.xjtu.edu.cn

[1] State Key Laboratory for Mechanical Behavior of Materials, School of Materials Science and Engineering, Shaanxi Province, Xi'an Jiaotong University, Xi'an 710049, People's Republic of China

Published online: 20 September 2024

5, 6, 7, 8). It is true that the oxide inclusions in the metal coatings are inevitable as the spraying is operating in open air. Although they are able to increase the hardness and thereby the wear resistance of the coatings (Ref 9, 10, 11), in most cases, the oxide inclusions result in the formation of unbonded intersplat interfaces. The properties and performance of thermal spray metal coatings are usually degraded. The oxide inclusions could also lead to discontinuity of local compositions and properties such as thermal expansion mismatching between metal alloy and oxide. When the coatings are operated at certain high temperature, the dismatching may cause premature debonding or delamination, and subsequently premature failure upon thermal cycling. Additionally, it cuts off the transportation passages for primary particles such as charges or element atoms. Accordingly, the thermal or electrical conductance will be reduced. Moreover, the diffusion of metal atoms will be also hindered such as in the bond coat for thermal barrier coatings (TBCs) which may degrade the stability of thermally grown oxide (TGO) in TBCs system and subsequently cause premature failure of TBCs.

Generally, when metal spray coating is carried out in an open ambient atmosphere, the oxidation is inevitable. The oxide inclusions in thermal spray metal coating arise from two stages: in-flight stage of spray particles in ambient atmosphere and post-impact deposition stage (Ref 12, 13). Based on the time scales of different physical processes involved in spray coating deposition from powder particle in-flight to spreading followed by rapid solidification and cooling, the former occurs in milliseconds, while the later occurs in several seconds. Up to now, numerous efforts have been made to prevent the oxidation of metals during thermal spraying through the development of different thermal spray processes and the optimization of spray parameters for individual processes. A comprehensive review on the oxidation of metals during thermal spraying has been given by Gan and Berndt (Ref 13). Among all thermal spray processes including flame spraying, arc spraying, plasma spraying, detonation gun spraying (D-Gun spraying), high velocity oxy-fuel spraying (HVOF), high velocity air-fuel spraying (HVAF) and vacuum plasma spraying, only using VPS (also referred to as LPPS, low-pressure plasma spraying) can avoid the oxidation of metals, since the metal spraying is carried out in a chamber with an inert atmosphere without oxygen.

It has been reported that when plasma spraying is carried out in open ambient atmosphere air will be enrolled into plasma jet (Ref 14). At a spray distance of 50 mm from the nozzle exit, the enrolled air takes over 50% of plasma gas (Ref 15). A further rapid increase in air content takes place with increase in spray distance. With HVOF flame jet, Hackett and Settles (Ref 16) indicated the intense entrainment of the surrounding atmosphere into HVOF jet. They reported that at a spray distance of 80 mm, the jet is entirely composed of combustion products, and at a typical spray distance of 400 mm, the centerline composition of the jet is nearly 20% atmosphere oxygen. Accordingly, within the substantial in-flight distance of spray particles, they are propelled by the flame jet enriching in air. Despite the oxidizing feature of the flame jet, the in-flight oxidation of metal spray particles may not occur significantly (Ref 16) when metal particle temperature is lower than the melting point of spray materials (Ref 17). Hanson and Settles (Ref 17) reported that when spray particle temperature is lower than the melting point of spray material the oxygen content in HVOF 316L stainless steel coatings deposited by the powders with a size of $39 \pm 9\mu m$ is lower, being at a level of about 0.25wt% independent on particle temperature, although it was attributed to the in-flight oxidation of 316L spray particles. However, when the particle temperature is higher than the melting point of spray particles the oxygen content in the coating increases significantly with the increase in spray particle temperature. Since the temperature of metal spray particles generated by gas-fueled HVOF process is generally higher than their melting points (Ref 18-20) and higher than those that are generated by liquid-fueled HVOF, gas-fueled HVOF metal coatings contain higher amount of oxides inclusions (Ref 18, 20). The oxygen content in gas-fueled HVOF metal coatings is higher than those by liquid-fueled HVOF metal coatings (Ref 21). Moreover, the oxygen content resulting from the in-flight oxidation is exponentially inversely proportional to spray particle size (Ref 12). When spray particle size is smaller than 50 μm, the oxygen content in the coating can be mainly attributed to the in-flight oxidation. Accordingly, as far as metal spray particles are heated to certain high temperature with partial melting or full melting, the significant in-flight oxidation is inevitable. Thus, only when metal coating deposition is carried out via solid particle impact, the significant in-flight oxidation of metal particles can be suppressed (Ref 17). Such finding is coincident with the common feature that cold spraying can effectively suppress the oxidation of spray particles. However, it was also found that the deposition efficiency was significantly reduced to lower than 20% when 316L particle temperature was about 100 °C lower than solidus (Ref 17). Therefore, practically taking account of wide spray particle size distribution and small-sized particles used in HVOF, it is generally difficult to suppress the oxidation even during HVOF through controlling particle temperature to just below its melting point. A certain amount of oxide inclusions in HVOF metal coatings were generally reported (Ref 12, 18-21). When HVAF with a further lower temperature flame than HVOF is used for metal coating, the spray particles in a small size range are generally used to increase the deposition

efficiency. The size effects on particle heating make the surface temperature of small-sized particles easily exceed their melting points and thus the oxide inclusions are present also in HVAF metal coatings (Ref 22, 23).

Therefore, the oxidation of in-flight molten metal droplets begins beyond the spray distance where the surrounding air is engulfed into the flame jet. Then, since the oxidation of in-flight metal spray particles continuously occurs, one important fact is that the resultant oxide inclusion and subsequently oxygen content in the coating increase cumulatively with the increase in the spray distance (Ref 24-28). All these factors which lead to oxide concentrating on part of the droplet surface or entangling into the inner of droplet will promote the oxidation due to more fresh metal surface exposed to surrounding atmosphere. Moreover, the oxygen content resulting from the in-flight oxidation is exponentially inversely proportional to spray particle size (Ref 12). When spray particle size is larger than 50 μm, the oxygen content in the coating can be mainly attributed to the post-impact oxidation. Therefore, to limit the oxide inclusion, metal spray powders of large size are preferable and they are used for air plasma spraying in industrial practice. However, with increase in spray particle size, the temperature of spray particles decreases and even becomes not fully molten. The particle velocity is also reduced due to large drag resistance. As a result, it becomes difficult to deposit a dense metal coating.

The post-impact oxidation depends on the surface temperature of flattened molten splats and their cooling process (Ref 16). The higher the temperature is, the oxidation becomes more intensive. Generally, with increase in spray distance the heating effect of flames to the substrate or coating surface is reduced and subsequently the post-impact oxidation becomes less severe. Consequently, the oxygen content resulting from the post-impact oxidation decreases with the increase in the spray distance (Ref 16). Fortunately, the post-impact oxidation could be weakened through the extra cooling such as compressed air cooling or even dry ice cooling. Therefore, different cooling techniques were developed to suppress the post-impact oxidation (Ref 29, 30). However, since individual metal splats are inevitably exposed to air atmosphere, a thin oxide scale in several nanometers to tens nanometers thick is evolved on the splat surface which hinders the metallurgical bonding formation between adjacent metal splats (Ref 31). As a result, it is well known that thermal spray metal coatings present a lamellar structure with limited lamellar interface bonding (Ref 32), which degrades the mechanical performances of the coatings significantly.

To minimize the in-flight oxidation during plasma spraying of metal coatings, many different measures have been taken such as using shrouding nozzle, optimizing spray conditions and selecting large size powders as summarized by Gan and Berndt in their review paper (Ref 13). However, it is still difficult to completely avoid the in-flight oxidation of metal droplets when plasma spraying of metal coatings is carried out in open atmosphere. It was recently found to be an effective approach to suppress the in-flight oxidation of alloying elements in molten spray particles during plasma spraying through development of effective strategies utilizing the deoxidizers as reported by Zeng et al. (Ref 33, 34). Zeng et al. compared the oxygen contents of APS Ni20Cr coating and NiCrBSiC coatings and they found that the oxygen content in APS NiCrBSiC coating is much lower than APS Ni20Cr coating (Ref 33). Accordingly, the deoxidizing effect during in-flight by the elements such as B, Si and C in NiCrBSiC powder was proposed since all those elements can be used as deoxidizers for the spray-fusing of self-fluxing alloys. The deoxidizing effects were further confirmed evidently by deliberately adding B and Si to pure iron (Ref 34), and however, oxide-free molten droplets were not achieved during APS in the investigation mentioned above since the results showed that the oxygen contents in the APS-sprayed deoxidizer-containing FeB and FeSi alloy coatings increased with the spray distance. By taking account of both the effects of thermodynamics and kinetics on the in-flight molten particle deoxidization by deoxidizers discussed in the following section, the strategy was proposed for generating the oxide-free metallic molten droplets by APS in ambient atmosphere (Ref 4). In this invited paper, the recent progresses on the in situ in-flight deoxidizing effect through powder design using deoxidizers will be presented based on our results published in recent papers.

Theoretical Basis for the In situ In-flight Deoxidization of Molten Metal Droplets

The theoretical basis for the in situ in-flight deoxidization includes thermodynamics concerning with the preferential oxidation of deoxidizer element rather than all other alloy elements in the molten droplets and kinetics for continuous oxidation of the deoxidizer with instantaneous gasification of resultant oxide. To suppress the oxidation of metallic elements in molten droplets through the oxidation of deoxidizers, the thermodynamic conditions should be fulfilled. Figure 1 shows Gibbs free energy of oxide formation against temperature for typical metals and boron as deoxidizer as well as carbon to form CO. These data in Ellingham diagrams were calculated based on the thermophysical properties reported in literature (Ref 35). Those data are primarily consistent with that reported in other literature (Ref 33, 36). It can be found that for the alloys including elements Fe, Cu, Ni, Co, Cr and Mn, the formation energy of their oxides is higher than that of boron oxide. Therefore, thermodynamically, the boron can be

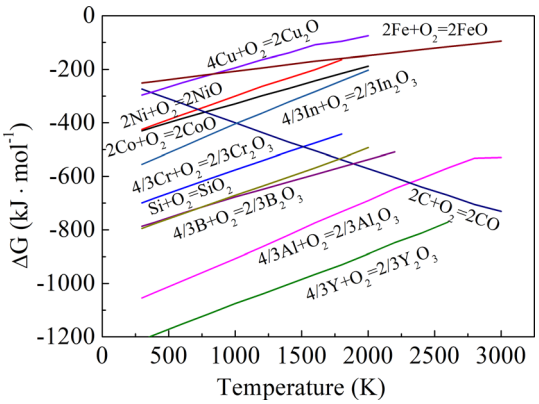

Fig. 1 Change of Gibbs free energy of oxide formation against the temperature for typical metals and boron as deoxidizer as well as carbon to form CO

used as the deoxidizer to prevent those elements from oxidation. Since the formation energy of SiO_2 is close to that of boron oxide, Si can also be used as deoxidizer as boron to prevent the metal elements from oxidation (Ref 33, 34). Moreover, it was reported that the formation of SiO (g) is favored over that of SiO_2 (s) at a temperature lower than 1786 °C (Ref 33), while SiO_2 has a high melting point and boiling point. Therefore, if silicon is used as the deoxidizer, to effectively deoxidize the metal droplets by silicon their temperatures should be kept lower than 1786 °C.

It can be also noticed from Fig. 1 that when metallic spray particles contain the elements whose oxide formation energy is lower than that of boron such as Al carbon can be used as the deoxidizer. In this case, the temperature of droplets must exceed 2007 °C. Therefore, to generate certainly high superhot spray particles becomes the necessary thermodynamic condition specially with the deoxidizer carbon.

To achieve oxide-free molten metallic droplets in ambient atmosphere, not only the thermodynamics conditions mentioned above must be fulfilled, but also the resultant oxide should be gasified rapidly to leave the droplet surface. B_2O_3 has a lower melting point of 450 °C than all the elements which can be reduced by boron. It is at a molten state in molten metal droplets. Accordingly, the resultant B_2O_3 tends to vaporize to deoxidize in molten droplet. In this case, deoxidizing effect depends on the temperature of droplets since vaporization rate of molten B_2O_3 increases with droplet temperature. It can be noticed that the boiling point of B_2O_3 is about 1860 °C. Moreover, the formation energy of B_2O_3 at its boiling point is close to its evaporation heat. Therefore, those facts mean that when the droplets having boron are heated to a temperature higher than the boiling point of B_2O_3, the resultant B_2O_3 can be evaporated instantaneously. Therefore, to ensure the

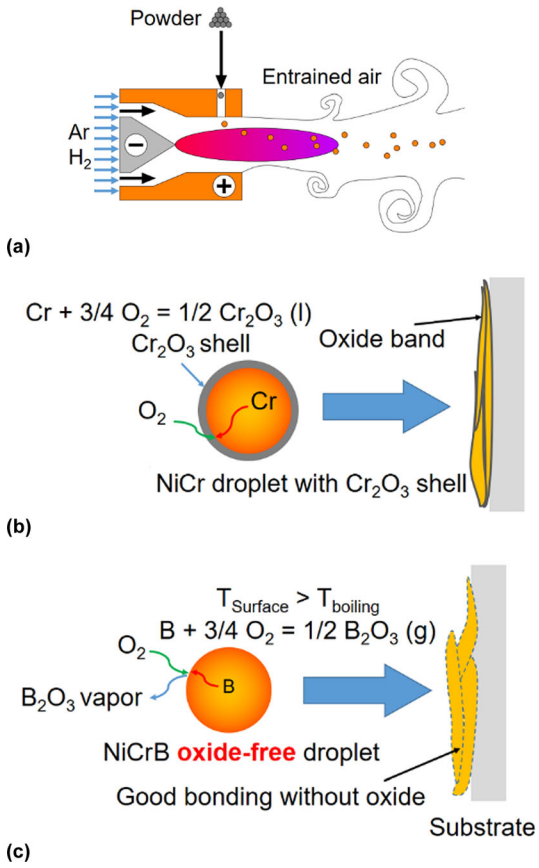

Fig. 2 Schematic diagram of air-entraining into plasma jet to generate an oxidizing plasma (a), Cr oxide formation on NiCr droplet surface representing conventional droplet without deoxidizer (b) and deoxidizing of molten NiCrB droplet by boron as a deoxidizer through its oxidation and B_2O_3 evaporation (c)

deoxidizing effect and remove oxide from droplet completely, it is necessary to heat the metal droplets to a temperature higher than the evaporation temperature of resultant oxides. For boron oxide, this temperature is equal to its boiling point. On the other hand, with deoxidizer silicon when the droplet temperature is higher than 1786 °C, the resultant SiO_2 becomes difficult to remove. While with the carbon there is no critical issue for removal of oxidation products from in-flight droplet since it reacts with oxygen to form gaseous CO.

Another condition concerned with the in situ deoxidization is the mass transfer rate of the deoxidizer within individual molten droplets. To maintain an oxide-free state for molten metallic droplets during the whole in-flight process prior to their impacts on the substrate in ambient atmosphere, the continuous reaction of the deoxidizer with the oxygen surrounding molten droplet surface has to be maintained. As shown schematically in Fig. 2, since the oxidation occurs continuously only at the surface of molten droplets, the deoxidization reduces the deoxidizer concentration near the droplet surface layer which may lead to

a deficiency of the deoxidizer. The diffusion of the deoxidizer from the inner toward droplet surface may supply the necessary deoxidizer. Too low concentration of the deoxidizer ignites the oxidation of other elements. To avoid the oxidation of other alloying elements, the deoxidizer should be transferred rapidly from the inner of the droplet toward its surface. Compared with the diffusion-controlled mechanism with a slow rate, the quick-rate convection mass transfer mechanism is required for the flying droplets which can be realized by initiating the Vortex motion within the droplet (Ref 37). Therefore, to maintain the kinetics for deoxidizing reaction the quick mass transfer mechanism within molten droplet and rapid removal of the resultant oxide through rapid gasification are necessary conditions. For rapid mass transfer, the interaction of in-flight molten droplets with plasma jet needs to ensure the convection mass transfer mechanism during in-flight. On the other hand, the droplet temperature which is higher than the boiling point of boron oxide ensures the rapid removal of the oxide from in-flight particles.

Materials and Methodology

The spray materials used for examining the in-flight in situ deoxidization by boron as the deoxidizer included two types of Cu-based spray powders (Ref 38, 39) and two types of Ni-based powders (Ref 40, 41). In those materials, alloying elements cover a wide range of Gibbs free energy for their oxide formation over the line for boron oxidation seen in Fig. 1. The Gibbs free energies of those elements for their oxide formation are higher than that of the boron oxide formation. With such powder design, the experiments may prove a broad feasibility of the in situ in-flight deoxidization mechanism using deoxidizer boron. Moreover, with carbon as the deoxidizer for Al-containing alloys, two aluminide powders of FeAl (Ref 42) and NiAl (Ref 43), and NiCrAlY (Ref 44) as typical MCrAlY powders were used. Except CuNiIn and NiCr powders without deoxidizer which were commercial powders for comparison, all other powders with adding boron or carbon were the powders designed for the present study. The most powders were used in a nominal spray particle size range from 30 to 50 μm. However, when the powders in other particle size ranges were used for comparison their particle size range will be noted additionally. The Cu-based and Ni-based powders using boron as a deoxidizer were manufactured by gas atomization process. With carbon deoxidizer for Al-containing materials, the diamond particles were used as carbon source. FeAl and NiAl, and Fe/Al/diamond and Ni/Al/diamond, NiCrAlY/diamond composite powders were prepared by the ball milling process. Commercial Fe powders, Ni powders, Al powders or NiCrAlY powders, which are available for thermal spraying, and diamond powder with a size range from 1 to 2 μm were used as the raw materials. Table 1 shows the nominal compositions of spray powders. For more details of the spray powders, the previous publications can be referred as shown in Table 1.

The oxygen content of the coatings was measured by oxygen, nitrogen and hydrogen analyzer (LECO TC-400 for oxygen, USA). The carbon contents of the powders and coatings were measured by carbon/sulfur analyzer (Elementrac CS-520, Eltra, Germany). The content of B was measured by inductively coupled plasma mass spectrometry (ICP-MS, NexION 350D, PerkinElmer, USA) with a precision of 0.01 wt.%. With all above measurements, the free-standing coatings detached from substrates were used. The particle surface temperature during in-flight was measured by a commercial thermal spray particle property diagnostic system (DPV-2000, Tecnar Automation Ltd, Canada) against spray distance.

Results and Discussion

In-flight In situ Deoxidizing of Metallic Droplets Along Flying Trajectory

Figure 3 and 4 shows typical results of droplet temperatures for the spray particles containing boron or carbon, respectively. It was found that within the spray distance range from 70 mm to 200 mm the temperature of molten spray particles tends to decrease with the increase in the spray distance (Ref 41, 42). The mean temperatures are also influenced by the particle size distribution and the composition of spray materials. Since the proportion of small particles in NiCrCu1.5 powders with D10 of 28.3 μm, D50 of 39.8 and D90 of 56.0 μm is higher than NiCrCu4B powders with D10 of 32.2 μm, D50 of 42.8μm and D90 of 57.1 μm, the NiCrCu1.5 powder particles presented a little more rapid decrease in temperature with the increase in the spray distance (Ref 41). This difference in particle temperature is possibly attributed to the fact that the particles having a relative smaller powder particle size loss the heat more rapidly during in-flight by heat convection and radiation due to higher specific surface area. The Fe-Al-C composite powder particles showed a lower temperature due to the low boiling point of Al (Ref 42). However, the measurement results revealed that with the spray particles using two different deoxidizers of boron and carbon in this project the thermodynamic conditions were all well fulfilled.

For the Cu-based alloys and Ni-based alloys mentioned above, boron is used as the deoxidizer. Figure 5 and 6 shows the effect of spray distance on the oxygen content of

Table 1 Compositions of spray powders used in the study (wt.%)

Spray powders	Ni/Fe	Cu	Cr	Al	In	B	C	Ref.
CuNiIn	31.84	63.5			4.30			38
CuNi4B	32.0	64.0				4.0		38
CuNiIn2B	62.00	36.54			3.40	1.40		39
CuNiIn4B	63.05	30.81			3.20	2.94		39
NiCr	80	20						40
NiCr4B	77		19			4.00		40
NiCrCu1.5B	62.5	22.5	13.8			1.2		41
NiCrCu3B	60.2	22.8	14.3			2.70		41
NiCrCu4B	60.4	21.9	13.8			3.90		41
FeAl2.5C	66.5			31			2.5	42
NiAlC	67.0			31.0			2.0	43
NiCrAlYC*	68.00		22.94	4.92			3.6	44

*: Y: 0.54 wt.%.

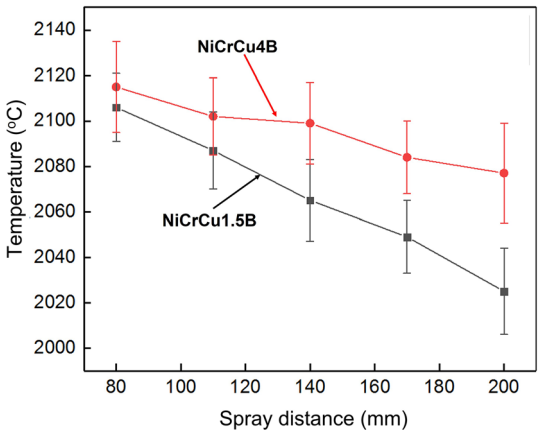

Fig. 3 Evolution of NiCrCuB spray particle temperatures during in-flight along spray distance (Ref 41). Reprinted with permission of Thermal Spray Technology

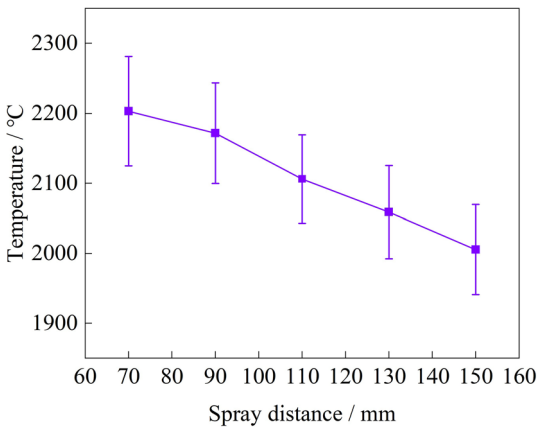

Fig. 4 Evolution of FeAl2.5C spray particle temperature during in-flight along spray distance (Ref 42). Reprinted with permission of China Surface Engineering

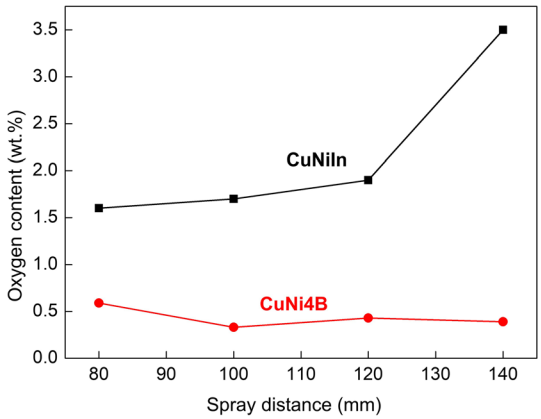

Fig. 5 Change of the oxygen content in CuNi4B coating with the spray distance in comparison with the conventional APS CuNiIn coating (Ref 38). Reprinted with permission of Acta Metallurgica Sinica

the APS-sprayed CuNiB and NiCr coatings as the typical Cu-based alloy and Ni-based alloy, respectively. The experiments were made in compared with the conventional CuNiIn and Ni20Cr alloy coatings, respectively. The measurement of spray particle temperature confirmed that the droplet temperature is higher than 2000 °C (Ref 38, 40, 41) which fulfills the thermodynamics and kinetics conditions for boron to protect alloying elements from oxidation and resultant B_2O_3 to remove instantaneously (Ref 38, 40). For the conventional APS CuNiIn and NiCr coatings, their oxygen contents increased with the spray distance as reported (Ref 23-27). In contrast, with the CuNi and NiCr alloys containing 4 wt.% of boron, the oxygen contents in the coatings were reduced to much lower levels (Ref 38, 40). Those levels are comparable to or lower than that resulted from post-impact induced oxygen content

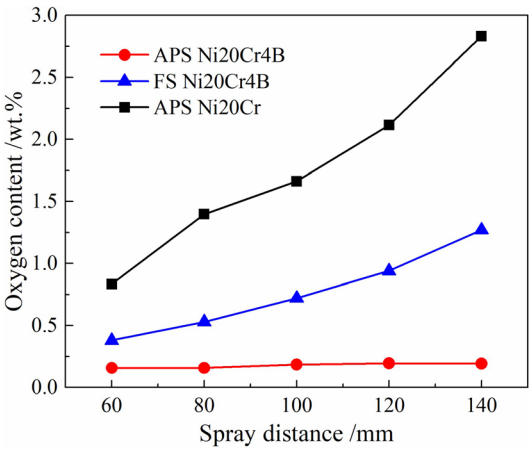

Fig. 6 Change of the oxygen content in APS NiCrB coating with the spray distance in comparison with flame-sprayed NiCrB coating, and the conventional APS Ni20Cr coatings (Ref 40). Reprinted from Ref 40, available under CC BY-NC-ND 4.0 license at ScienceDirect

levels. Another important fact is that the oxygen contents in the coatings decreased or increased little with the increase in the spray distance. This fact clearly indicates that the molten spray particles were flying in an oxide-free state due to sufficient deoxidizing effect of boron. Further examination into oxide inclusion in individual molten droplets by collecting spray particles passing through plasma jet showed no evident oxide both on the surface and inner of the sprayed CuNiIn2B particles as exhibited in Fig. 7 (Ref 39). The EDS analysis results from the surface and cross sections of collected powder particles confirm the state of oxide on two different powders (Table 2). With Ni20Cr4B powders, the coatings were also deposited by flame spraying which could only heat the spray particles to a mean temperature less than 1600 °C (Ref 40). As seen from Fig. 6, the oxygen content in the coatings increased with the increase in the spray distance. Although vaporization of molten B_2O_3 occurs during in-flight, this fact may indicate that the vaporization even at a high temperature is not enough to rapidly remove all oxide. Therefore, the formation of the deoxidizer oxide in gas phase is necessary to achieve oxide-free molten metal droplets during thermal spray in the open atmosphere.

Figure 8 shows the oxygen content in the APS-sprayed FeAlC coating with the FeAl powders containing 2.5 wt.%C against the spray distance in compared with that of the APS FeAl coatings. In this case, the diamond particles in a size range of 1-2 μm were added into ball-milled FeAl particles as deoxidizer. The oxygen content in APS FeAlC coatings decreased from 1.01 wt.% at 70 mm to 0.48 wt.% at 150 mm with the increase in the spray distance from 70 mm to 150 mm (Ref 42). On the contrary, the oxygen contents in the APS FeAl coatings increased from 3.38 wt.% at 70 mm to 4.15 wt.% at 150 mm. The results reveal that both the Fe and Al can be protected from oxidation during the whole in-flight process and their in-flight oxidation was completely suppressed. In particular, the addition of diamond as deoxidizer can effectively protect aluminum element from oxidation. This was also confirmed by APS of NiAl (Ref 43) and NiCrAlY coatings (Ref 44).

Effect of Deoxidizer Content in Molten Droplets on the Deoxidizing Behavior

The effect of the deoxidizer content in spray particles on the deoxidizing effect was investigated using the powders with different deoxidizer contents. Figure 9(a) shows the oxygen contents in the APS NiCuNiB coatings deposited using the NiCuB powders of different boron contents against the spray distance. It was found that with the NiCu4B powders containing the boron from 3 wt.% to 4 wt.%, the oxygen content in the coatings decreased with the increase in the spray distance (Ref 41). Thus, the oxygen content in the coating was determined by post-impact oxidation. While with the NiCuCrB powders containing 1.5wt.% boron, the oxygen content in the coatings tended to decrease with the increase in the spray distance from 80 mm to 100 mm and then turned to increase with a further increase in the spray distance (Ref 41). This fact means that during in-flight of spray particles further far from 100 mm the in-flight oxidation of spray particles began to take place. The examination into the change of the boron content of in-flight spray particles reveals that the boron content may have a minimum threshold to effectively protect alloying element from oxidation (Fig. 9b). The results suggest that 0.5 wt% of boron could be the critical level below which the in-flight oxidation of spray particles occurs. This was also evident from the results of CuNiIn2B and CuNiIn4B coatings (Fig. 10) (Ref 38). It can be found from Fig. 10(a) and (b) that when the boron content is reduced to less than 0.5 wt.% the oxygen content in the CuNiB coating turns to increase with spray distance from the decreasing tendency. It should be noticed that the effective utilization of deoxidizer depends on the transfer of the deoxidizer inside molten particle toward its surface region. The faster the mass transfer rate toward droplet surface, the lower the minimum deoxidizer content becomes.

For APS NiAl coatings, the coating deposited using Ni/Al/ composite spray powders from 30-50 μm gave the oxygen content of 3.23 wt.% at a spray distance of 80 mm (Ref 43). When 2wt.% diamond was added into Ni/Al/C composite powder, the oxygen content of the NiAlC coating was reduced to 0.61 wt.% (Ref 43). Here, the NiAlC refers to the NiAl splat or coating deposited using Ni/Al/C composite powders. Figure 11 exhibits the oxygen content of APS NiAlC coatings against the spray distance.

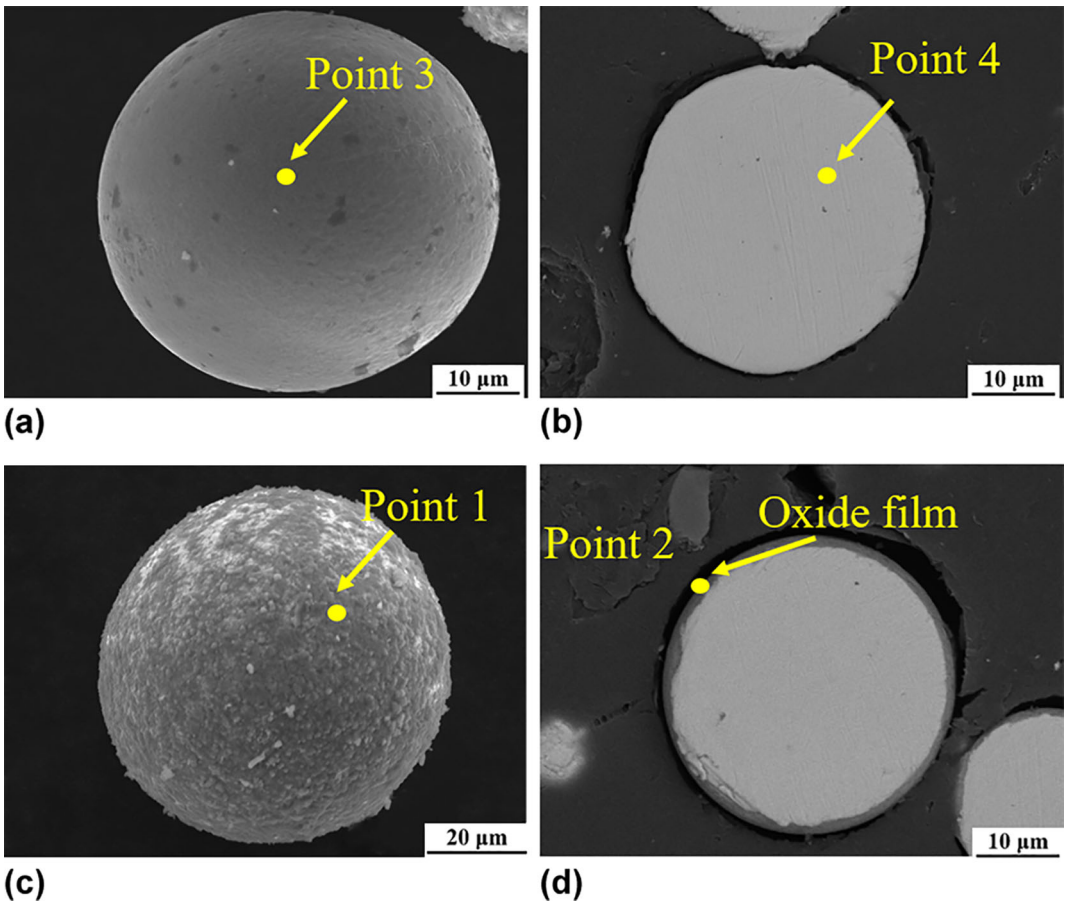

Fig. 7 Comparison of surface morphology and cross-sectional microstructure of CuNiIn2B sprayed particles experienced heating by plasma jet in ambient atmosphere (a, b) with conventional CuNiIn sprayed powder particle (c, d) (Ref 39). Reprinted from Surface and Coatings Technology, Vol. 464, Yong-Sheng Zhu, Xiao-Tao Luo, Yin-Qiu Sun, Yuan Ren, Chang-Jiu Li, Atmospheric plasma-sprayed CuNiInB coatings of high fretting wear performance enabled by oxide-free metallic droplet deposition, p. 129537, Copyright 2023, with permission from Elsevier

Table 2 The EDS analysis results at the points marked in Fig. 7

Element	Point 1 (at.%)	Point 2 (at.%)	Point 3 (at.%)	Point 4 (at.%)
Cu	19.54	0.16	59.92	52.96
Ni	31.05	27.56	35.74	44.06
In	0.24	0.02	0.20	0.08
O	49.17	72.26	4.14	2.90
Total	100.00	100.00	100.00	100.00

This result suggests that the in-flight oxidation of NiAlC particles occurred evidently at the spray distance far from 80 mm. Taking account of residual carbon content in the coating shown in Fig. 12, the critical carbon content is a little higher than 0.6wt% for NiAl droplets. This fact implies that the minimum carbon content is higher than the minimum boron content. It is reasonable when the fact is considered that one boron atom takes one and a half oxygen atoms on average while one carbon atom consumes only one oxygen atom upon oxidation. From this perspective, a critical carbon content of about 0.83% could be estimated (Ref 43). However, the examination into the results for FeAlC coating (Fig. 8) revealed that even the carbon content is reduced to less than 0.5wt.% it is still effective to protect Al and Fe from in-flight oxidation (Ref 42). Those facts suggest that the physical property of molten droplets influences significantly the oxidation of the deoxidizer possibly due to the change of mass transfer rate. This is because the melting points of NiAlC and FeAlC are significantly different (Ref 45). The large difference results in big difference in over-heating temperature than the melting points since the droplet temperatures of both the

NiAlC and FeAlC are comparable. Since residual deoxidizer will be left in the coatings as alloying element, its minimum content should be acceptable for service of the final alloy coatings.

The Particle Size Effect on Deoxidation

A previous study revealed that the oxygen content resulted from in-flight oxidation increases exponentially to the reciprocal of the spray particle size (Ref 12). Thus, the in-flight oxidation becomes severe as the spray particle size is reduced. For spray molten particles with the same particle size distribution which have the same content of deoxidizer, since the deoxidizer in smaller spray particle is consumed more rapidly, the deoxidizer content in smaller particles decreases more rapidly during in-flight. When the deoxidizer content reduces to a level below the critical value as discussed above, the deoxidizer provides only partial protection. As a result, the in-flight oxidation of other alloy elements becomes severe gradually. Figure 13 shows the NiAlC splats typically for different sizes deposited at three different spray distances using the Ni/Al/C composite powders containing 2.5wt% diamond as carbon deoxidizer in a size range of 30-50 μm. It was recognized that there was no evident oxide block attached to large splats deposited at 80 mm (Ref 43). However, several small oxide blocks appeared on the splat deposited with small droplets. It was attributed to low carbon content in small droplet since the severe oxidation of small particle consumes more deoxidizer and results in deficiency of deoxidizer in the smaller droplet more quickly. When the spray distance was increased over 80 mm, the carbon content in the spray particles reduced to a level less than 0.5 wt.% (Fig. 12), the oxidation of alloy elements in larger particles also occurred to result in oxide blocks attaching on splat surface. Evidently, more oxide blocks were attached to smaller splats and those deposited at a longer spray distance. All those results further reveal that the certain level of deoxidizer content in in-flight spray particles, in particular for small particles, should be maintained to keep the oxide-free state during the whole in-flight range prior to impact on substrate.

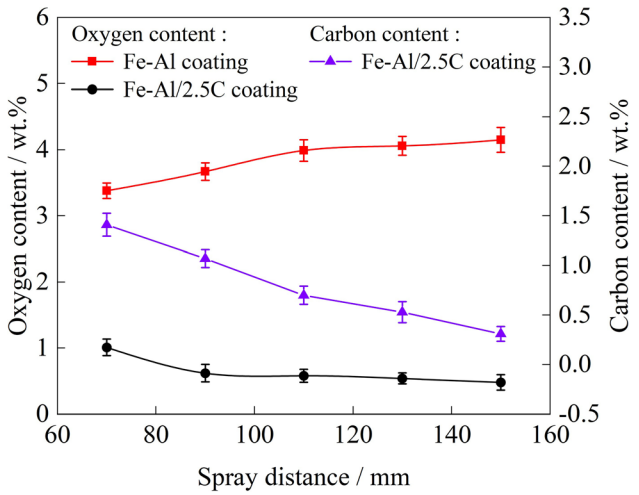

Fig. 8 Change of the oxygen content in APS FeAlC coating with the spray distance in comparison with the conventional APS FeAl coating along with the carbon content in the sprayed FeAlC coating (Ref 42). Reprinted with permission of China Surface Engineering

Effect of the Post-impact Oxidation on Oxygen Content

The above-mentioned results revealed that with proper design of the metallic feedstock powders having certain

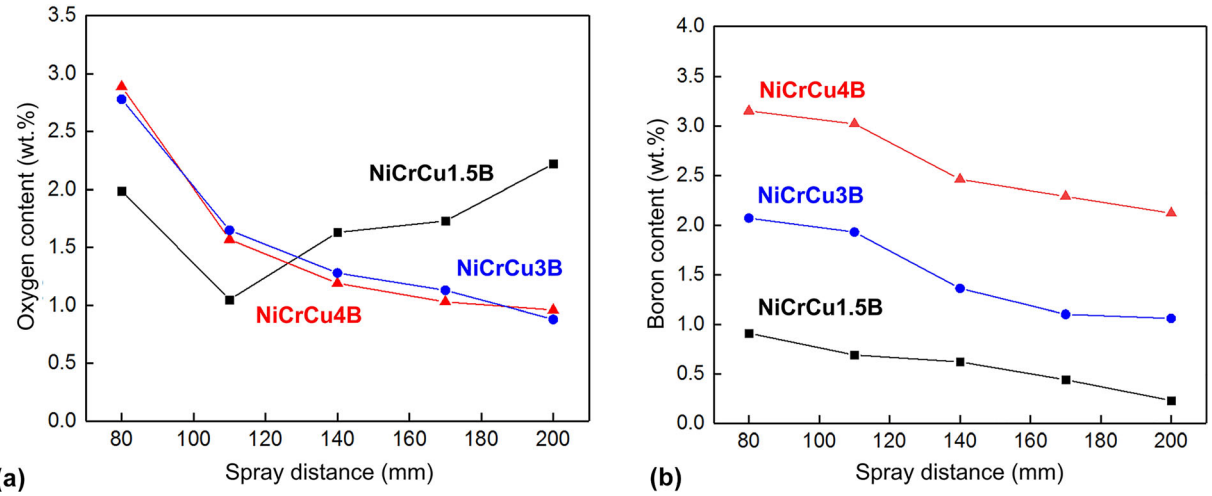

Fig. 9 Effect of the boron content on the dependency of the oxygen content in APS NiCrCuB coating on the spray distance (a) and change of the boron content in APS NiCrCuB coatings with the spray distance for three spray powders of different boron contents (Ref 41). Reprinted with permission of Thermal Spray Technology

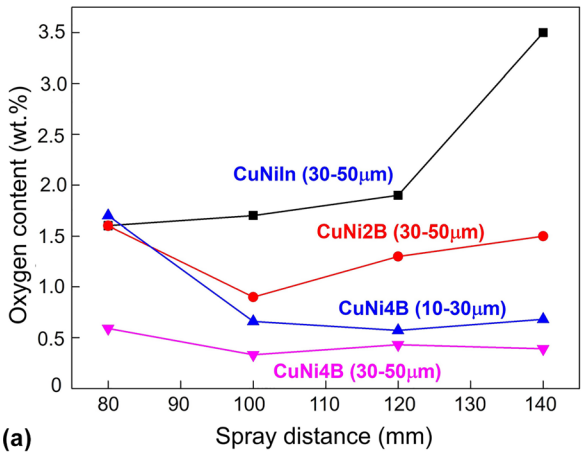

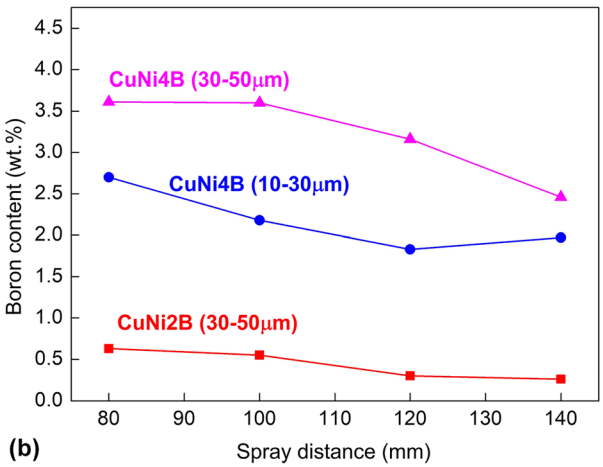

Fig. 10 Effect of the boron content on the dependency of the oxygen content in APS CuNiB coating on spray distance in comparison with APS CuNiIn coating (a) and change of the boron content in APS CuNiB coatings with the spray distance for three spray powders of different boron contents and particle sizes (Ref 38). Reprinted with permission of Acta Metallurgica Sinica

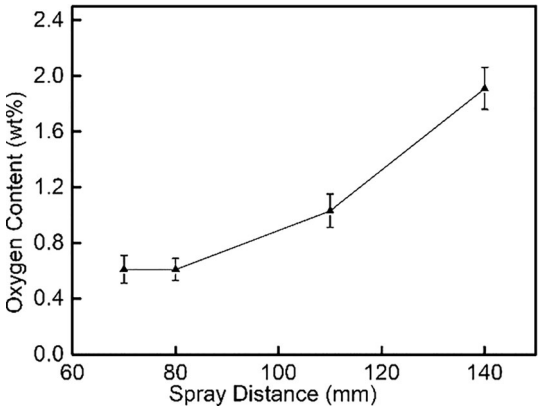

Fig. 11 Change of the oxygen content in APS NiAlC coating with the spray distance (Ref 43). Reprinted from Journal of Materials Processing Technology, Vol. 319, Li Zhang, M. Mahrukh, Di Wang, Xian-Jin Liao, Xiao-Tao Luo, Chang-Jiu Li, Oxidation protection dynamics of NiAl droplet by in-flight in situ carbon deoxidation during atmospheric plasma spraying for high-performance NiAl coatings, p. 118088, Copyright 2023, with permission from Elsevier

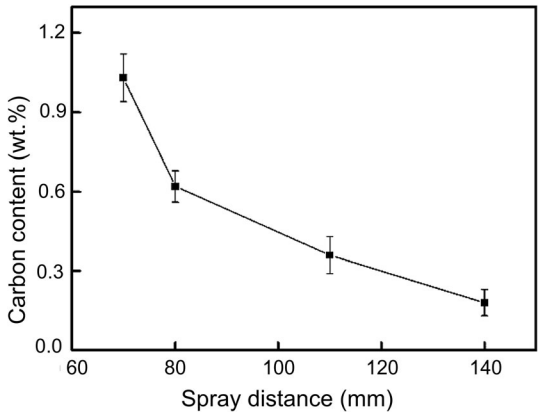

Fig. 12 Change of the carbon content in APS NiAlC coating with the spray distance (Ref 43). Reprinted from Journal of Materials Processing Technology, Vol. 319, Li Zhang, M. Mahrukh, Di Wang, Xian-Jin Liao, Xiao-Tao Luo, Chang-Jiu Li, Oxidation protection dynamics of NiAl droplet by in-flight in situ carbon deoxidation during atmospheric plasma spraying for high-performance NiAl coatings, p. 118088, Copyright 2023, with permission from Elsevier

amount of deoxidizer the in-flight oxidation of molten metal droplets can be completely suppressed. This means that by APS the oxide-free molten metal droplets can be generated in ambient atmosphere. However, the post-impact oxidation cannot be avoided. It is generally accepted that with the forced cooling of sprayed coating the post-impact oxidation can be significantly limited. Figure 14 shows the oxygen content of the APS NiCuCr4B coatings against the spray distance deposited under the conditions with and without the backside cooling of spray samples by an air jet. It can be seen that the oxygen contents of the coatings under two conditions decreased with the increase in the spray distance since the coatings were deposited by the same oxide-free molten NiCuCrB spray particles. The oxygen detected in the coatings was introduced by the post-impact oxidation. It is clear that when the spray coating was subjected to the forced cooling from the backside of substrate during spraying, the oxygen content in the coating was significantly reduced. At a spray distance of 110 mm, the oxygen content was reduced from over 1.5 wt.% to about 1 wt.%, and to a level less than 0.75 wt% with further increase in spray distance to 170 mm (Ref 41). Therefore, the present data evidently demonstrate that the post-impact oxidation can be significantly suppressed by proper cooling measures during thermal spraying.

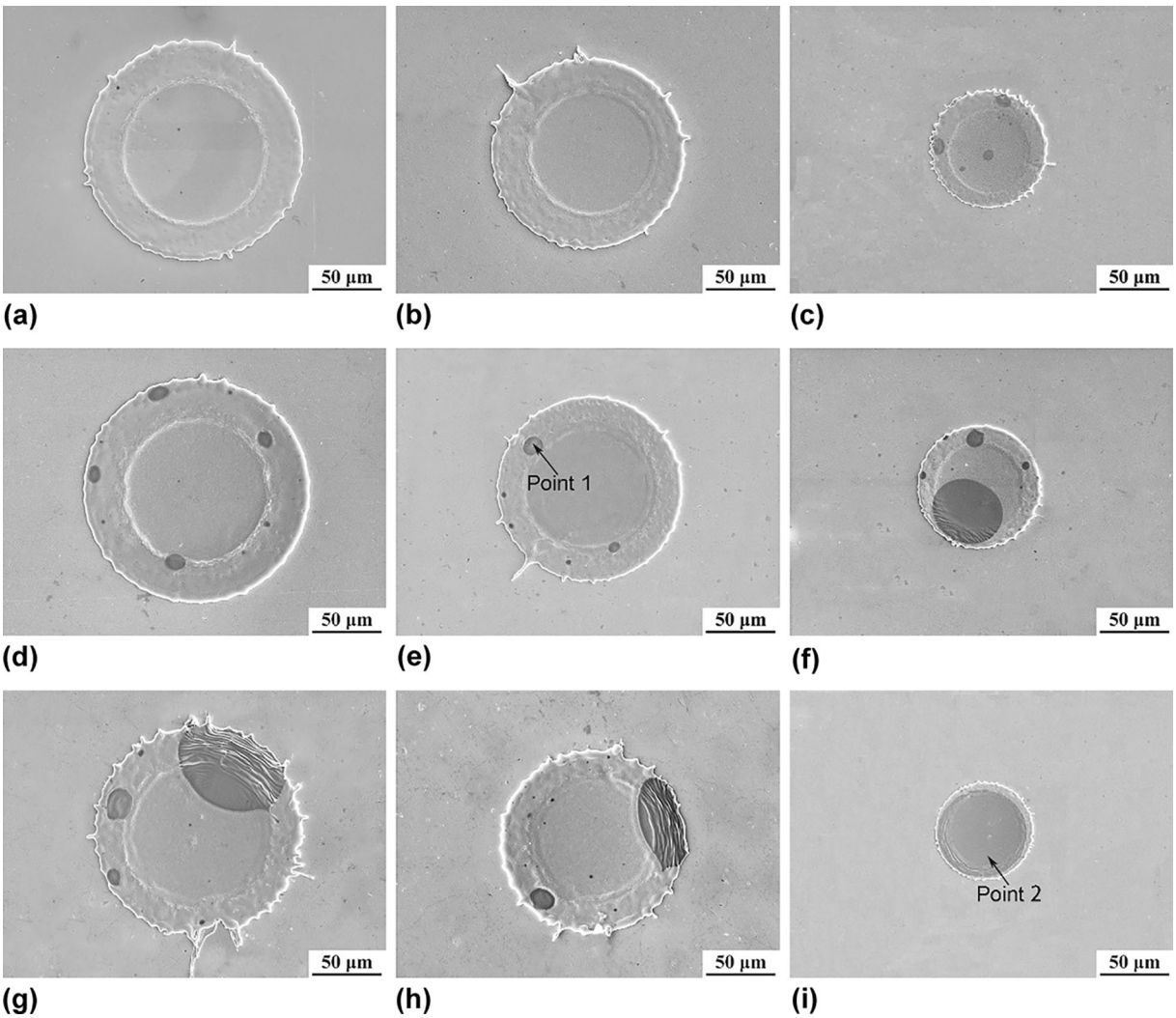

Fig. 13 Typical NiAl splats of different sizes APS-deposited at different spray distances using Ni/Al-2.5C composite powders: 80 mm (a, b, and c), 110 mm (d, e and f), and 140 mm (g, h and i). The regions with a black contrast on splat surface exhibit the oxide attached to splat surface (Ref 43). Reprinted from Journal of Materials Processing Technology, Vol. 319, Li Zhang, M. Mahrukh, Di Wang, Xian-Jin Liao, Xiao-Tao Luo, Chang-Jiu Li, Oxidation protection dynamics of NiAl droplet by in-flight in situ carbon deoxidation during atmospheric plasma spraying for high-performance NiAl coatings, p. 118088, Copyright 2023, with permission from Elsevier

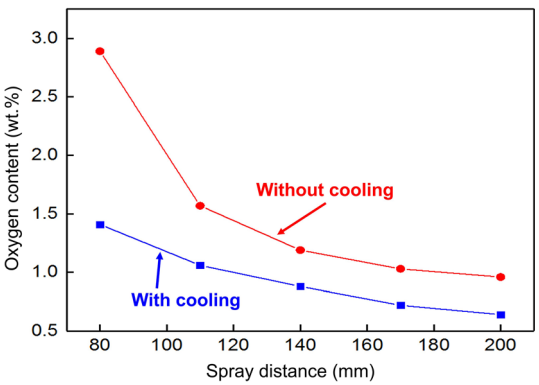

Fig. 14 Effect of substrate cooling on the dependency of the oxygen content in APS NiCrCu4B coating with the spray distance (Ref 41). Reprinted with permission of Thermal Spray Technology

Effect of In situ Deoxidizing on Microstructure and Property of the Coatings

The suppression of the in-flight oxidation of molten metal spray particles creating oxide-free spray metal particles brings about significant impact on the microstructure of thermal spray metal coatings. The absence of blocky oxide inclusions improves the wettability of spreading metal melt to deposited splats and thus possibly intersplat bonding. Adding boron as deoxidizer can also reduce the melting point of the alloys. This further enhances the possibility of metallurgical bonding formation across the intersplat boundaries. Figure 15 compares the microstructure of the APS conventional Ni20Cr coating with that of the APS NiCr4B coating. Since spray particles in a small size range

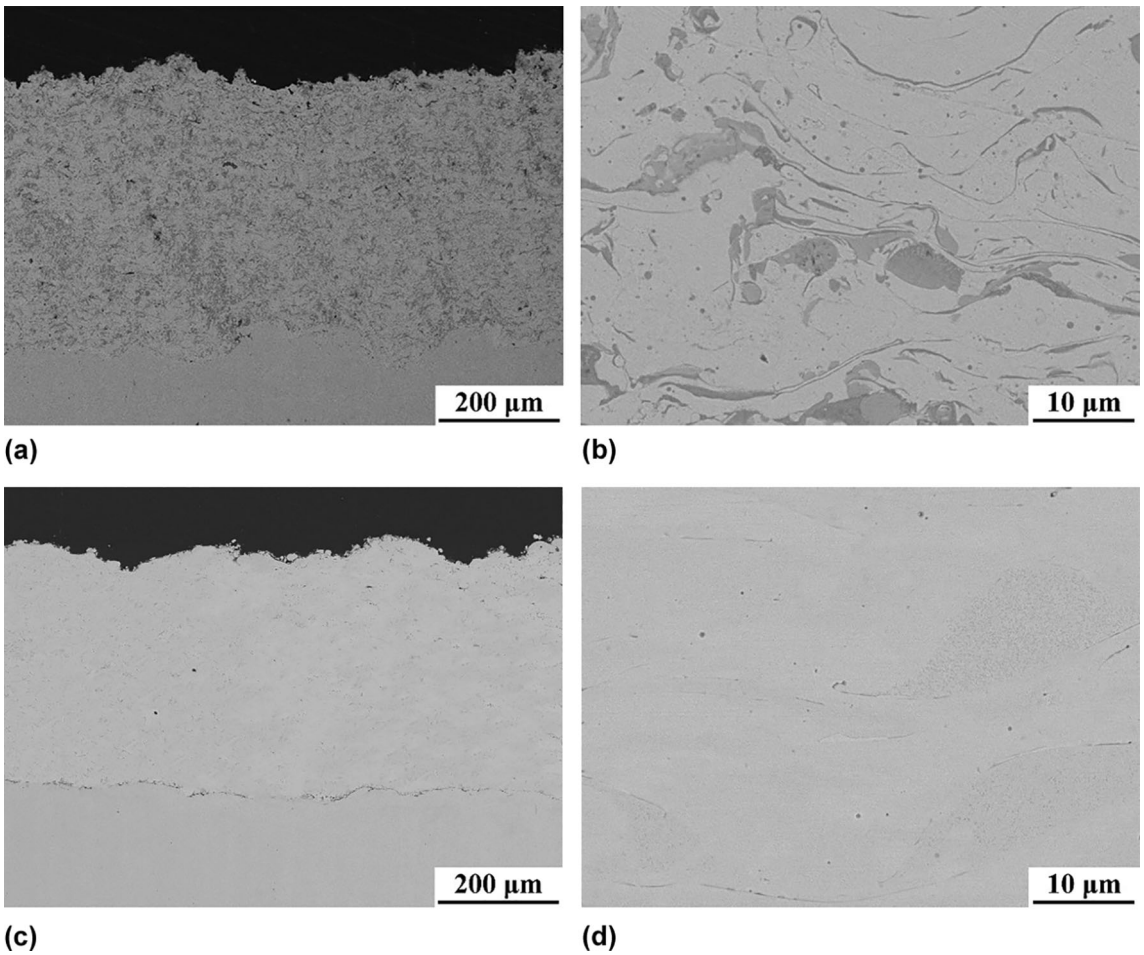

Fig. 15 Comparison of the microstructure of APS Ni20Cr coating (a, b) with that of APS NiCr4B coating (c, d) (Ref 40) Reprinted from Ref 40, available under CC BY-NC-ND 4.0 license at ScienceDirect

from 30 to 50 µm were used, the severe in-flight oxidation of spray Ni20Cr particles resulted in large inclusion of oxides in the coating. A large amount of oxide inclusions degrade the intersplat bonding which results in substantial unbonded splat interfaces. All those unbonded interfaces are interconnected to permit the corrosive substance to penetrate through the coatings. On the other hand, NiCrB coating presents a dense microstructure without evident oxides as shown in Fig. 15 (c) and (d).

Figure 16 shows the microstructure of the APS CuNiB coating deposited on stainless steel with its cross section etched using aqua regia. It can be found that even though significant etching occurred to splats themselves no any preferential corrosion occurred to the intersplat interfaces in the coating, which indicates metallurgical bonding formation at the adjacent intersplat boundaries. Therefore, the addition of boron as the deoxidizer could also promote intersplat bonding. Moreover, the residual boron in the coatings forms nickel borides to increase the coating hardness significantly. Figure 17 shows the effect of the boron content in the APS CuNiB coating on its microhardness. The coating hardness increases proportionally to the boron content in the coating. Therefore, based on the boron content design the coating hardness and then the wear performance can be controlled.

Thereafter, molten salt corrosion test (Ref 40) and long-term immersion corrosion test in the mimic ocean water (Ref 46) were carried out to examine the corrosion resistance of the APS NiCrB coatings which were used as model coating. Figure 18(a) shows the weight gain of the Ni20C4B coating against the test time due to corrosion in comparison with those of bare stainless steel substrate and the conventional Ni20Cr coating sprayed stainless steel samples (Ref 40). It is clearly shown that the Ni20Cr4B coating sprayed sample presents excellent corrosion resistance. The examination into the cross-sectional microstructure after the test revealed that the APS Ni20Cr coating spalled off the substrate due to the corrosion at the interface between the coating and substrate by the salt penetrating through the coating (Fig. 18b). On the other hand, with the Ni20Cr4B coating the corrosion occurred only at the surface region of the coating and without any

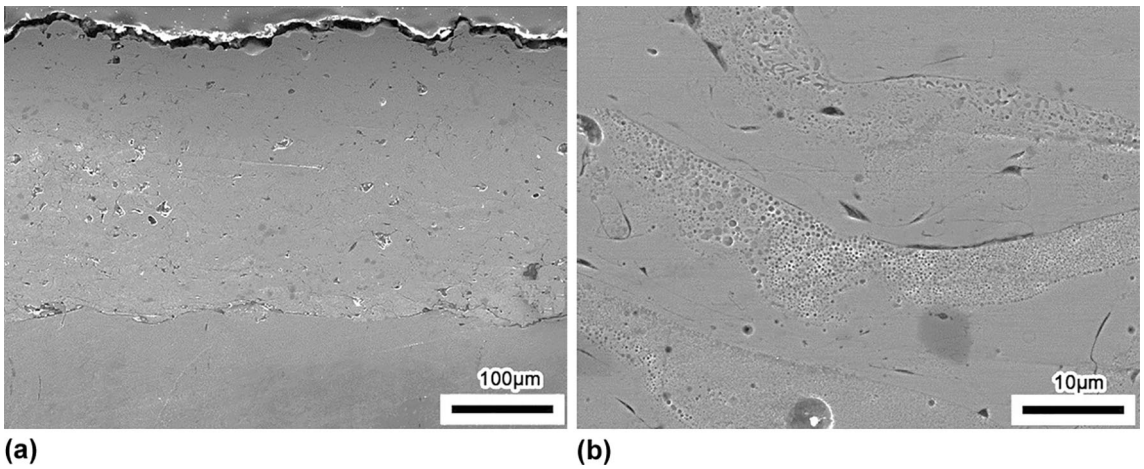

Fig. 16 Microstructure of APS CuNi4B coating with cross section etched by aqua regia solution to reveal the interface bonding at different magnifications (Ref 38). Reprinted with permission of Acta Metallurgica Sinica

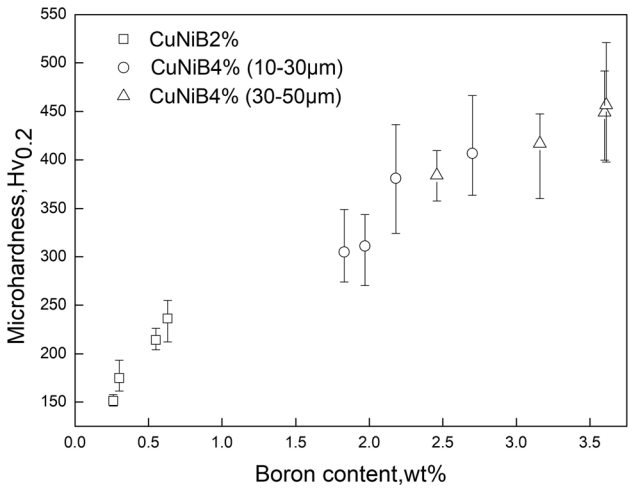

Fig. 17 The relationship between the microhardness of APS CuNiB coating and its boron content (Ref 38). Reprinted with permission of Acta Metallurgica Sinica

trace of molten salt penetration (Fig. 18c). In order to examine the protection of the APS NiCr4B coating against the penetration of aqueous solution which has a much lower viscosity than molten salt, the Ni20Cr4B coating was deposited on Al alloy for immersion test in 3.5%NaCl solution since Al alloy has a much lower potential than Ni-based alloy. Figure 19(a) shows the change of the open circuit potential of the sample against the immersion time. It was revealed that during 80 days immersion the potential of the Ni20Cr4B coating is close to that of the spray-fused NiCrBSi alloy which is higher than Al substrate alloy and no any decrease in potential toward that of the substrate was observed (Ref 46). The examination to the microstructure of the coated Al alloy showed no change after immersion for 80 days as shown in Fig. 19 (b) and (c). Those corrosion test approved that the NiCrB coating is solution-tight not to permit the corrosive substance to penetrate through the coating.

Figure 20 compares the microstructure of the APS FeAl coating in comparison with that of APS FeAl2.5C coating. Due to the effective in-flight deoxidizing, the addition of diamond as deoxidizer reduced significantly the oxide inclusions in the coating. The coating porosity was reduced from 2.7% for the APS FeAl coating to 0.33% for the FeAl2.5C coating. The addition of carbon leads to formation of carbide in the coating which increases the coating hardness from less than 300 Hv for APS FeAl coating to about 600 Hv for FeAlC. Figure 21 shows the microstructure of APS NiAl2C coating in comparison with that of the conventional APS NiAl coating (Ref 43). A large number of oxides were present in the conventional NiAl coating which reduce significantly active Al amount when the coating is used at high temperature oxidation atmosphere. The NiAl2C coating not only presented a dense microstructure with much less oxide inclusions, but also improved intersplat bonding. Thus, when the NiAl2C coating was directly exposed to high temperature oxidation, the self-healing of intersplat boundaries occurred resulting in the formation of a continuous protective α-Al_2O_3 oxide layer on the coating surface (Ref 47). When carbon was added into NiCrAlY powders as deoxidizer, a dense NiCrAlY coating with few oxides was deposited by APS as shown in Fig. 22 (Ref 44). During high temperature exposure the residual carbon in the coating is precipitated uniformly as Cr_7C_3. Certain amount of carbide will effectively reduce thermal expansion coefficient (Ref 48). Therefore, the high performance of MCrAlY coatings can be deposited cost-effectively by APS through designing MCrAlY powders to have carbon deoxidizer.

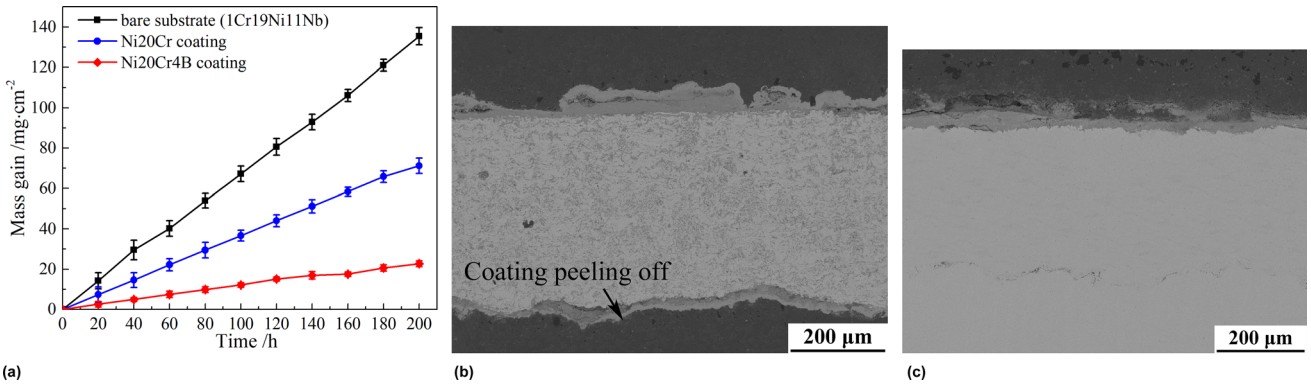

Fig. 18 Change of the weight gain of Ni20C4B coating against the test time due to molten salt corrosion in comparison with those of bare stainless steel substrate and Ni20Cr coating sprayed stainless steel samples (a), the cross-sectional microstructures of the coated stainless steel samples with APS Ni20Cr coating (b) and Ni20Cr4B coating (c) after salt corrosion test (Ref 40) Reprinted from Ref 40, available under CC BY-NC-ND 4.0 license at ScienceDirect

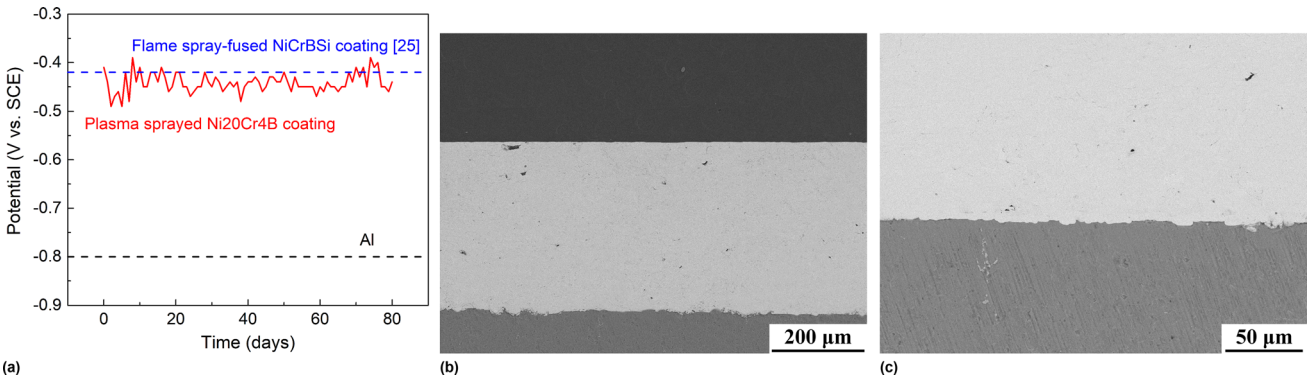

Fig. 19 Change of the natural potential of the Ni20Cr4B APS-sprayed Al alloy (ZAlSi7Mg) immersed in 3.5% NaCl solution (a) and coating microstructure after 80 days immersion test (b, c) (Adapted from Ref 46). Reprinted with permission of ASM International. All rights reserved. www.asminternational.org

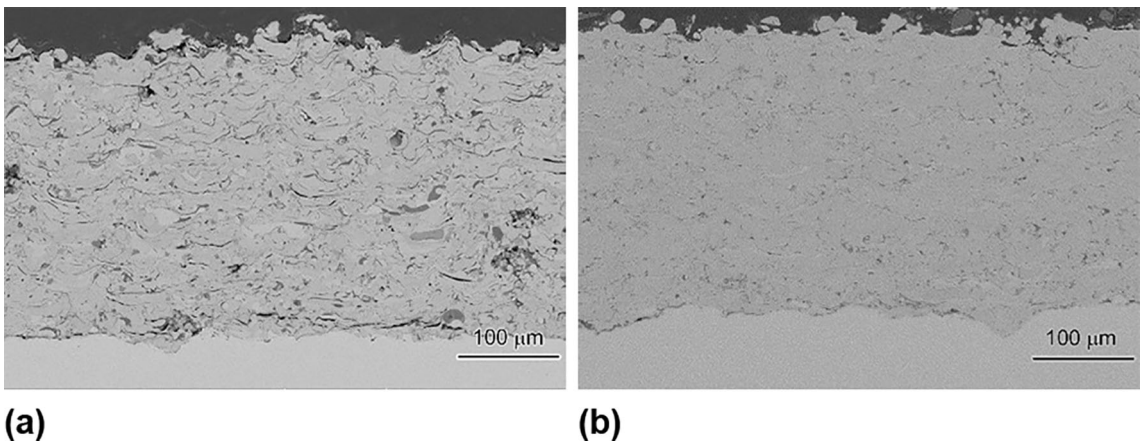

Fig. 20 Comparison of APS FeAl coating (a) with ASP FeAl2.5C coatings (b) (Ref 42). Reprinted with permission of China Surface Engineering

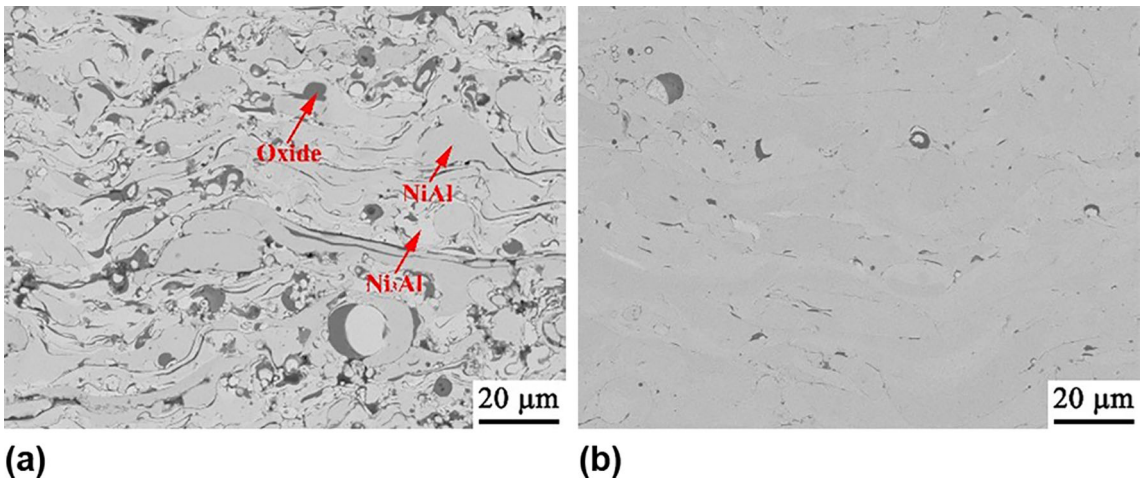

Fig. 21 Comparison of conventional ASP NiAl coating (a) with APS NiAl2C coating (b)

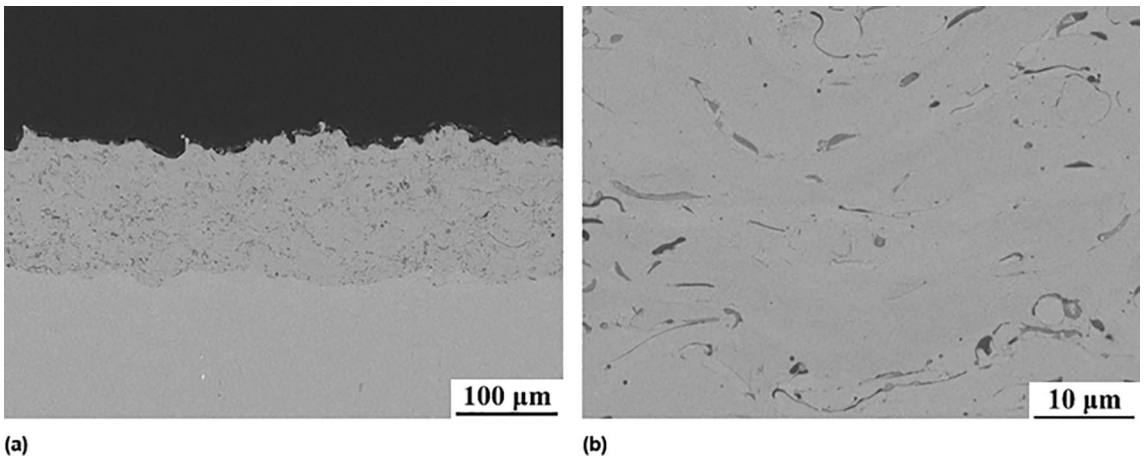

Fig. 22 Microstructure of APS NiCrAlY4C coating showing the minimized oxide inclusions

Conclusions

Depending on whether the alloys contain Al element or not, the boron or carbon can be added into thermal spray powders as deoxidizer. The molten droplets of high temperatures, which fulfill the deoxidizing thermodynamics conditions, can be generated by air plasma spraying. The in-flight oxidation of alloying elements in molten spray metal droplets can be completely suppressed. The coatings deposited by those droplets presented significantly lower oxygen contents as compared with the counterparts without deoxidizer. Moreover, the oxygen contents in individual coatings decrease with the increase in the spray distance. The oxygen content in the APS metal coatings is attributed to the post-impact oxidation of molten droplets. It becomes possible to achieve oxide-free molten metal spray particles in the ambient atmosphere through designing spray metal powders to contain the deoxidizers. The results also suggested that for certain metallic particles, there exists a minimum threshold deoxidizer content for complete deoxidization during the whole in-flight period. Moreover, the particle size effects on the consumption of deoxidizer and, heat and mass transfer behavior should be taken into consideration to design the spray powders and optimize the spray conditions. It was well demonstrated that using oxide-free molten droplets which have a superhot temperature the high-performance metal coatings can be cost-effectively deposited by APS which is promising for expanding the application fields of APS.

Acknowledgments The present project is financially supported by the Key Program of the National Nature Science Foundations of China (No.52031010, No. U1837201), and National Science and Technology Major Project (2019-VII-0007-0147).

References

1. P. Fauchais, J.V.R Heberlain, and M.I. Boulos, Thermal Spray Fundamentals From Powder to Part, Springer (New York, 2014). https://doi.org/10.1007/978-0-387-68991-3.
2. J.R. Davis, Handbook of Thermal Spray Technology, (ASM International, Materials Park, 2004)
3. A. Vardelle, C. Moreau, and J. Akedo The 2016 Thermal Spray Roadmap, *J. Therm. Spray Technol.*, 2016, **25**(8), p 1376-1440.
4. C.-J. Li, X.T. Luo, X.Y. Dong, L. Zhang, and C.X. Li, Recent Research Advances in Plasma Spraying of Bulk-like Dense Metal Coatings with Metallurgically Bonded Lamellae, *J. Therm. Spray Technol.*, 2022, **31**(1), p 5-27.
5. L. Zhang, X.-J. Liao, S.-L. Zhang, X.-T. Luo, and C.-J. Li, Effect of Powder Particle Size and Spray Parameters on the Ni/Al Reaction During Plasma Spraying of Ni-Al Composite Powders, *J. Therm. Spray Technol.*, 2021, **30**(1-2), p 181-195. https://doi.org/10.1007/s11666-020-01150-2
6. J.J. Song, X.Y. Dong, J.W. Tian, X.T. Luo, and C.-J. Li, The Adhesive Strength of the Novel Bond Coat Deposited by Atmospheric Plasma Spraying Using Mo-clad Ni20Cr Powders, *Therm. Spray Technol.*, 2022, **14**(4), p 19-28. ((**In Chinese**))
7. S. Shinde and S. Sampath, A Critical Analysis of the Tensile Adhesion Test for Thermally Sprayed Coatings, *J. Therm. Spray Technol.*, 2022, **31**, p 2247-2279.
8. C.-J. Li, J.-J. Song, X.-T. Luo, X.-Y. Dong, and L. Zhang, A novel bond coat with excellent adhesive strength by plasma-spraying of Mo-clad core-shell-structured metal powders, Thermal Spray 2023: Proceedings from the International Thermal Spray Conference, May 22-25, 2023; Quebec City, Canada; https://doi.org/10.31399/asm.cp.itsc2023p0344
9. R.C. Tucker, Structure Property Relationships in Deposits Produced by Plasma Spray and Detonation GUN TECHNIQUES, *J. Vac. Sci. Technol.*, 1974, **11**(4), p 725-734.
10. S.E. Hartfifield-Wunsch and S.C. Tung, The Effect of Microstructure on the Wear Behavior of Thermal Spray Coatings, Thermal Spray Industrial Applications, C.C. Berndt and S. Sampath, Ed., ASM International, Materials Park, 1994, p 19-24
11. K. Dobler, H. Kreye and R. Schwetzke, Oxidation of Stainless Steel in the High Velocity Oxy-fuel Process, *J. Therm. Spray Technol.*, 2000, **9**(3), p 407-413.
12. C.-J. Li and W.-Y. Li, Effect of Sprayed Powder Particle Size on the Oxidation Behavior of MCrAlY Materials During HVOF Deposition, *Surf. Coat. Technol.*, 2003, **162**, p 21-41.
13. J.A. Gan and C.C. Berndt, Review on the Oxidation of Metallic Thermal Sprayed Coatings: A Case Study with Reference to Rare-earth Permanent Magnetic Coatings, *J. Therm. Spray Technol.*, 2013, **22**, p 1069-1091.
14. J. Miyase, Thermal Spray Handbook, Japan Thermal Spray Association, Auto-Press, 1998, p.21 (In Japanese)
15. J.R. Fincke, D.M. Crawford, S.C. Snyder, W.D. Swank, D.C. Haggard, and R.L. Williamson, Entrainment in High-velocity, High-temperature Plasma Jets, *Part I: Exp Results, Heat and Mass Transfer*, 2003, **46**, p 4201-4213.
16. C.M. Hackett and G.S. Settles, Turbulent Mixing of the HVOF Thermal Spray and Coating Oxidation, Thermal Spray Industrial Applications, C.C. Berndt and S. Sampath, Ed., ASM International, Materials Park, 1994, p 307-312 (No. 19)
17. T.C. Hanson and G.S. Settles, Particle Temperature and Velocity Effects on the Porosity and Oxidation of an HVOF Corrosion-control Coating, *J. Thermal Spray Technol.*, 2003, **12**, p 403-415.
18. J. Saaedi, T.W. Coyle, H. Arabi, S. Mirdamadi, and J. Mostaghimi, Effects of HVOF Process Parameters on the Properties of Ni-Cr Coatings, *J. Thermal Spray Technol.*, 2010, **19**(3), p 521-530.
19. D. Zois, T. Wentz, R. Dey, S. Sampath, and C.M. Weyant, Simplified Model for Description of HVOF NiCr Coating Properties through Experimental Design and Diagnostic Measurements, *J. Thermal Spray Technol.*, 2013, **22**(2-3), p 299-315.
20. P. Patel, V.N.V. Munagala, N. Sharifi, A. Roy, S.A. Alidokht, M. Harfouche, M. Makowiec, P. Stoyanov, R.R. Chromik, and C. Moreau, Infuence of HVOF Spraying Parameters on Microstructure and Mechanical Properties of FeCrMnCoNi High-entropy Coatings (HECs), *J. Mater. Sci.*, 2024, **59**, p 4293-4323.
21. K. Dobler, H. Kreye, and R. Schwetzke, Oxidation of Stainless Steel in the High Velocity Oxy-fuel Process, *J. Thermal Spray Technol.*, 2000, **9**(3), p 407-413.
22. P. Khamsepour, J. Oberste-Berghaus, M. Aghasibeig, F. Ben Ettouil, A. Dolatabadi, and C. Moreau, The Effect of Spraying Parameters of the Inner-diameter Highvelocity Air-Fuel (ID-HVAF) Torch on Characteristics of Ti-6Al4V in-Flight Particles and Coatings Formed at Short Spraying Distances, *J. Thermal Spray Technol.*, 2023, **32**, p 568-585.
23. K. Bobzin, H. Heinemann, and K. Jasutyn, Numerical and Experimental Investigation for Application of CoNiCrAlY Coatings by HVAF, *J. Thermal Spray Technol.*, 2024, **33**, p 1167-1177.
24. T. Fukushima and S. Kuroda, Oxidation of HVOF Sprayed Alloy Coatings and Its Control by a Gas Shroud, Thermal Spray 2001: New Surfaces for a New Millennium, C.C. Berndt, K.A. Khor, and E.F. Lugscheider, Ed., ASM International, Materials Park, 2001, p 527-532.
25. A.A. Syed, A. Denoirjean, P. Fauchais, and J.C. Labbe, On the Oxidation of Stainless Steel Particles in the Plasma Jet, *Surf. Coat. Technol.*, 2006, **200**, p 4368-4382.
26. A.A. Syed, A. Denoirjean, P. Denoirjean, J.C. Labbe, and P. Fauchais, In-flight Oxidation of Stainless Steel Particles in Plasma Spraying, *J. Thermal Spray Technol.*, 2005, **14**, p 117-124.
27. Kuroda and S. Kitahara, Effects of Spray Conditions on the Pore Structure and Quenching Stress in Plasma Sprayed Coatings, Proceddings of International Thermal Spray Conference 1995, Kobe, Japan, (ed) A. Ohmori, High Temperature Society of Japan, p.489-494.
28. G. Espie, P. Fauchais, J.C. Labbe, A. Vardelle, and B. Hannoyer, Oxidation of Iron Particles during APS: Effect of the Process on Formed Oxide, Wetting of Droplets on Ceramic Substrate, Thermal Spray 2001: New Surfaces for a New Millennium (ed) C.C Berndt, K.A. Khor and E.F. Lugscheifer, ASM International, Materials Park, USA, 2001, p 821-827.
29. S.J. Dong, B. Song, B. Hansz, H.L. Liao, and C. Coddet, Improvement in the Properties of Plasma-sprayed Metallic, Alloy and Ceramic Coatings Using Dry-Ice Blasting, *Appl. Surf. Sci.*, 2011, **257**(24), p 10828-10833.
30. Z.J. Zhou, S.X. Song, W.Z. Yao, G. Pintsuk, J. Linke, S.Q. Guo, and C.C. Ge, Fabrication of thick W Coatings by Atmospheric Plasma Spraying and their Transient High Heat Loading Performance, *Fusion Eng. Des.*, 2010, **85**(10-12), p 1720-1723. https://doi.org/10.1016/j.fusengdes.2010.05.021
31. A. Valarezo and S. Sampath, An Integrated Assessment of Process-microstructure-property Relationships for Thermal-sprayed NiCr Coating, *J. Therm. Spray Technol.*, 2011, **20**(6), p 1244-1258.
32. J. Wang, X.-T. Luo, C.-J. Li, N. Ma, and M. Takahashi, Effect of Substrate Temperature on the Microstructure and Interface Bonding Formation of Plasma Sprayed Ni20Cr Splat, *Surf. Coat. Technol.*, 2019, **371**, p 36-46. https://doi.org/10.1016/j.surfcoat.2019.01.085
33. Z. Zeng, S. Kuroda, and H. Era, Comparison of Oxidation Behavior of Ni-20Cr Alloy and ni-base Self-fluxing Alloy During Air Plasma Spraying, *Surf. Coat. Technol.*, 2009, **204**, p 69-77.

34. Z. Zeng, S. Kuroda, J. Kawakita, M. Komatsu, and H. Era, Effects of Some Light Alloying Elements on the Oxidation Behavior of Fe and Ni-Cr Based Alloys During Air Plasma Spraying, *J. Therm. Spray Technol.*, 2010, **19**, p 128-136.
35. D.J. Ye and J.H. Hu, *Handbook of Practical Thermodynamic data*, Metallurgical Industry Press, Beijing, 2002. ((**In Chinese**))
36. M.S. Li, *High Temperature Oxidation of Metals*, Metallurgical Industry Press, Beijing, 2001. ((**In Chinese**))
37. S. Prakash and W.A. Sirignano, Liquid Fuel Droplet Heating with Internal Circulation, *Int. J. Heat Mass Tran.*, 1978, **21**(7), p 885-895. https://doi.org/10.1016/0017-9310(78)90180-1
38. Y. Ren, X.Y. Dong, H. Sun, X.T. Luo, C.X. Li, M. Mahrukh, and C.-J. Li, Oxide Cleaning Effect of In-flight CuNi Droplet During Atmospheric Plasma Spraying by B Addition and Its Influence on the Coating Composition and Structure, *Acta Metall. Sin.*, 2022, **58**(2), p 206-214. ((**In Chinese**))
39. Y.-S. Zhu, X.-T. Luo, Y.-Q. Sun, Y. Ren, and C.-J. Li, Atmospheric Plasma-sprayed CuNiInB Coatings of High Fretting Wear Performance Enabled by Oxide-free Metallic Droplet Deposition, *Surf. Coat. Technol.*, 2023, **464**, 129537.
40. X.Y. Dong, X.T. Luo, Y. Ge, and C.-J. Li, Enhancing the Hot-corrosion Resistance of Atmospheric Plasma Sprayed Ni-based Coatings by Adding a Deoxidizer, *Mater. Des.*, 2021, **211**, 110154.
41. H. Sun, X.Y. Dong, Y. Ren, X.T. Luo, C.X. Li, M. Mahrukh, and C.-J. Li, Influences of Spray Parameters and Powder Composition on the Coating Composition, Microstructure and Properties During Atmospheric Plasma Spraying of NiCrCuB, *J. Therm. Spray Technol.*, 2021, **13**(1), p 1-12. ((**in Chinese**))
42. Z. Zhou, L. Zhang, X.Y. Dong, X.T. Luo, and C.-J. Li, Effect of Diamond Addition in Powder on Removing Oxide and Enhancing Bonding Between Coating Particles in Atmospheric Plasma Spraying, *China Surface Eng.*, 2023, **36**(1), p 44-56. ((**In Chinese**))
43. L. Zhang, M. Mahrukh, D. Wang, X.J. Liao, X.T. Luo, and C.-J. Li, Oxidation Protection Dynamics of NiAl Droplet by Inflight In-situ Carbon Deoxidation During Atmospheric Plasma Spraying for High Performance NiAl Coatings, *J. Mater. Proc. Technol.*, 2023, **319**, 118088.
44. Y.-S. Zhu, X. Xue, X.-T. Luo, and C.-J. Li, Air plasma-sprayed MCrAlY coatings with low oxide content enabled by adding a deoxidizer, Proceedings of ITSC2024, ADVANCING THERMAL SPRAY TECHNOLOGY— Innovations, Applications and Sustainability, DVS, Germany, 2024 221-227.
45. Q.W. Guo, G.S. Wang, and G.C. Guo, *Phase Atlas for Common Nonferrous Alloys (Changyong Youse Jinshu Eryuanhejin Xiangtuji)*, Chemistry Industry Press, Beijing, 2009. **(in Chinese)**.
46. X.-Y. Dong, Y.-S. Zhu, X.-T. Luo, and C.-J. Li, Long-term corrosion behavior of atmospheric plasma sprayed NiCr alloy coating containing boron in 3.5 wt.% NaCl solution, Thermal Spray 2023: Proceedings from the International Thermal Spray Conference 2023; Quebec City, Canada; https://doi.org/10.31399/asm.cp.itsc2023p0730
47. L. Zhang, D. Wang, X.-J. Liao, R. Chen, X.-T. Luo, and C.-J. Li, Study on the Oxidation Resistance Mechanism of Self-healable NiAl Coating Deposited by Atmospheric Plasma Spraying, *Mater. Degradation*, 2023, **7**(1), p 62.
48. J. He, Advanced MCrAlY Alloys with Doubled TBC Lifetime, *Surf. Coat. Technol.*, 2022, **448**, 128931.

Publisher's Note Springer Nature remains neutral with regard to jurisdictional claims in published maps and institutional affiliations.

Springer Nature or its licensor (e.g. a society or other partner) holds exclusive rights to this article under a publishing agreement with the author(s) or other rightsholder(s); author self-archiving of the accepted manuscript version of this article is solely governed by the terms of such publishing agreement and applicable law.